Computational Materials Science 138 (2017) 288–294

Contents lists available at ScienceDirect

Computational Materials Science

journal homepage: www.elsevier.com/locate/commatsci

Promoting defect formation and microwave loss properties in δ-MnO_2 via Co doping: A first-principles study

Lulu Song, Yuping Duan *, Yahong Zhang, Tongmin Wang *

Key Laboratory of Solidification Control and Digital Preparation Technology (Liaoning Province), School of Materials Science and Engineering, Dalian University of Technology, Dalian 116085, PR China

ARTICLE INFO

Article history:
Received 23 March 2017
Received in revised form 14 June 2017
Accepted 15 June 2017

Keywords:
δ-MnO_2
Defects
Dielectric properties
Magnetic loss

ABSTRACT

The δ-MnO_2 has a layered structure and is expected to be a good absorbing material. Here, CASTEP was used for a theoretical study of the microwave absorption properties of δ-MnO_2 with defects (interstitial and substitutional cobalt atoms, vacancies). The results show that by analyzing the density of states (DOS) and partial density of states (PDOS), the defects change the charge distribution and increase the magnetic moment (increased by about 19 orders of magnitude). The bond length increased from 1.979 Å to 1.980 Å after substitutional defects formed to enhance the displacement polarizability. The changes in the charge distribution increase the atomic polarizability. The presence of crystal defects enhances both the magnetic loss and dielectric loss. In addition, the calculated defect formation energies show that the Co atoms tend to form interstitial atoms in MnO_2 (−16.90 eV), and the oxygen vacancy defects (−0.77 eV) are more easily formed than the manganese vacancy (33.14 eV).

1. Introduction

Manganese dioxide has been widely studied for many years due to its low cost and lack of toxicity. Manganese dioxide has great potential as a catalyst [1], electrode [2], absorber [3], etc. The formation mechanism of MnO_2 has been extensively researched. Manganese dioxide have several different crystalline phases. There are many research results into the morphological and electrochemical performance of MnO_2 [4–6]. When studied as a microwave absorbent, MnO_2 shows great performance in dielectric loss properties via Fe, Co, or Ni doping [7,8]. While the spontaneous magnetization of MnO_2 is almost zero, the magnetic loss is low. Experimental results show that the magnetic moment increased after magnetic ionic doping, but these studies are mostly based on α-MnO_2 and β-MnO_2.

Recently, theoretical calculations have become increasingly important. They are a credible way to predict materials properties and can predict electrochemical performance [9–11], chemical reactions [12], and other physical and chemical properties [13,14]. Pure elements [15], metal compounds [16–18], and organic matter [19] have all been studied. First-principles are also used in MnO_2 studies.

Tompsett et al. [20] studied the surface properties of β-MnO_2 by PBE + U to prove that it has potential as battery cathodes, catalysts and supercapacitors. Duan et al. studied the dielectric and electromagnetic properties of α-MnO_2 [21] and β-MnO_2 [22] after doping and vacancy formation. Yusuke et al. [23] researched the electronic states of four kinds of MnO_2 crystals (α-, β- δ- and λ-MnO_2), but did not consider the effect of the crystal defect. Kwon et al. [24] studied δ-MnO_2 with Ruetschi defects and identified the theoretical basis for enhanced photoconductivity. Similarly, most studies use α-MnO_2 and β-MnO_2. Thus far, there are few theoretical studies aiming at the microwave absorption properties of δ-MnO_2.

δ-MnO_2 is a MnO_2 with a layered structure that can be synthesized via a one-pot soft chemical reaction [25]. There are K^+ ions and H_2O molecules in the interlayer and this stabilizes the structure. Because of the special structure, δ-MnO_2 has good absorption capacity, and it can be used to absorb Cu^{2+}, Ni^{2+}, Zn^{2+}, Cd^{2+}, etc. These features can facilitate microwave absorption when the magnetic ions are contained in the interlayer.

Mn is a transition metal from the 4th period. Its electronic configuration is $3d^5 4s^2$. Mn in manganese dioxide is tetravalent, and its outermost electron shells are 3d shells that are partially filled. Mn has a permanent magnetic moment. Different configuration of [MnO_6] octahedras has different spin configuration, shown in Fig. 1. In microwave frequency, main magnetic loss specific mechanism are natural resonance and eddy current effect [26]. Eddy current effect (W_e) can be described as $W_e = CB_m^2$, where C is a

* Corresponding authors.
E-mail addresses: duanyp@dlut.edu.cn (Y. Duan), tmwang@dlut.edu.cn (T. Wang).

http://dx.doi.org/10.1016/j.commatsci.2017.06.020
0927-0256/

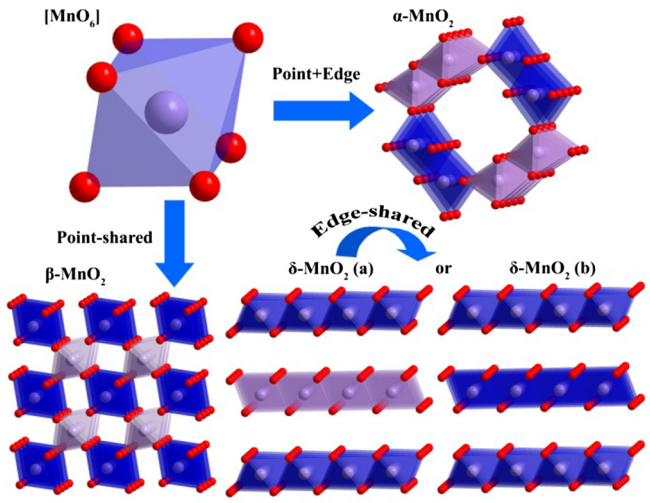

Fig. 1. [MnO_6] octahedra and the magnetic structure of α-, β-, and δ-MnO_2. The Mn atoms are purple and O are red. The blue and lavender octahedra represent the different spin directions. (For interpretation of the references to colour in this figure legend, the reader is referred to the web version of this article.)

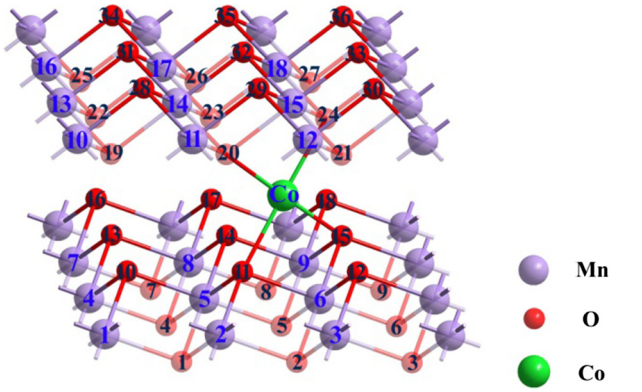

Fig. 2. Numbered atoms. The Mn atoms are purple, O are red, and Co are green. (For interpretation of the references to colour in this figure legend, the reader is referred to the web version of this article.)

value related with the frequency of electric field, the sample size and the resistivity. B_m is the magnetic induction intensity. B_m is proportional to applied magnetic field and magnetization intensity. Magnetization intensity is proportional to net magnetic moment. The net magnetic moment can be found from calculation method. The initial setup of spin configuration will influence the calculation results. According to the Goodenough-Kanamori rule, when two [MnO_6] octahedra share the same ridge and these two Mn atoms have the same spin directions—this Mn-Mn coupling is ferromagnetic (FM). When two [MnO_6] octahedra share the same point and these two Mn atoms have different spin directions, then this is called antiferromagnetic (AFM) [23]. The [MnO_6] octahedra are edge-shared in each layer of the δ-MnO_2. There are two kinds of spin configuration schemes, shown as Fig. 1 δ-MnO_2 (a) and (b). There is almost no energy difference between the FM and AFM configurations [23]. In the experimental situation, pure MnO_2 exhibited nonmagnetic character. So in this paper, spin configuration followed as δ-MnO_2 (a): each layer of δ-MnO_2 should be FM configured, and adjacent layers show AFM configuration.

In this paper, the dielectric and magnetic properties of δ-MnO_2 are discussed by first-principles calculations. Interionic electrostatic interactions are analyzed to explain the electromagnetic wave absorption mechanisms of δ-MnO_2. The influence of crystal defects on the microwave loss properties is discussed. This work complements previous theoretical studies on MnO_2.

2. Models and computational methods

The P-MnO_2 model is an ideal δ-MnO_2 supercell ($3 \times 3 \times 1$, Mn_8O_{16}). The model of δ-MnO_2 is determined as in the literature [27] (space group $P6_3/mmc$, a = b = 2.840 Å, c = 14.031 Å), which was layered MnO_2. There is no pure δ-MnO_2 in nature or even in the laboratory. Pure δ-MnO_2 is an ideal product. In order to simplify the calculation process, the interlayer K^+ and interlayer H_2O were moved from the crystal. The frame structure of δ-MnO_2 was retained. Although the model is different from the experimental results, it can also show the properties of δ-MnO_2 [24,28]. The atoms have been numbered as seen in Fig. 2.

This study contains five different models. Pure δ-MnO_2 ($Mn_{18}O_{36}$) is marked as P-MnO_2, and δ-MnO_2 with an extra Co atom (interstitials, $Mn_{18}CoO_{36}$) is marked as I-MnO_2. The δ-MnO_2 with a Co atom substituted for the Mn atom ($Mn_{17}CoO_{36}$) is marked as S-MnO_2, and the vacancy-O δ-MnO_2 ($Mn_{18}O_{35}$) is marked as v-O and vacancy-Mn δ-MnO_2 ($Mn_{17}O_{36}$) is marked as v-Mn. These models are shown in Fig. 3. The I-MnO_2 is formed by putting one Co atom in the P-MnO_2 crystal, and the doping site is one of the 6 h sites (Wyckoff position), which has been tested as shown in Fig. 3(b). The S-MnO_2 model (Fig. 3(c)) is built by replacing the No. 5 Mn atom with a Co atom, which based on P-MnO_2. The doping concentrations are 5.5 mol%. The initial spin states of the Co atom follow the states of the Mn atom that are replaced. The v-O (Fig. 3(d)) and v-Mn (Fig. 3(e)) are constructed by removing one O atom No. 14 and Mn atom No. 5 from P-MnO_2, respectively.

In this study, the CASTEP code [29]—which is based on the density functional theory (DFT) framework to probe the interactions and correlations of the series of solids based on the δ-MnO_2—and the plane wave basis is set; the ultrasoft pseudopotential was used. The Perdew Burke Ernzerhof (PBE) and generalized-gradient approximation (GGA) were also used. The GGA usually underestimates the band gaps of semiconductors. The local density approximation (LDA) was used with Hubbard U corrections (U-J) of 2.5 eV to 3d electrons (LSDA + U) [21]. The DFT + U was used to correct the van der Waals. After testing, a $4 \times 4 \times 2$ Monkhorst-Pack grid in the Brillouin zone and a 500 eV cutoff energy were used. Mulliken population analysis have been calculated to obtain the information about overlap population and Mulliken charges. In CASTEP, related calculation method has been described in previous papers [30]. The entire calculation process is carried out in the reciprocal space.

3. Results and discussion

After geometrical optimization, the lattice constants were changed. The relaxed lattice constants of the supercell ($3 \times 3 \times 1$, P-MnO_2) are a = b = 8.934 Å and c = 9.791 Å. The lattice constants of theoretical samples are different from the experimental samples. The value of c in particular is much smaller than the experimental one (14.03 Å). The differences may be due to the experimental samples that contain interlayer K^+ and interlayer H_2O. versus pure MnO_2, the lattice constants of defective structures have slight differences in the a-axis and b-axis, while the changes in c-axis are obvious. All defective models have different degrees of decrease in the c-axis. The contractions may be caused by the Jahn-Teller distortion [31].

3.1. Electronic structures and magnetic loss

Almost all properties of materials are caused by behavior of electrons [32]. The density of states (DOS) and partial density of